Title

A Rhenium Isonitrile Complex Induces Unfolded Protein Response-Mediated Apoptosis in Cancer Cells.

Journal

Chemistry - A European Journal, 25(39)

Authors

King, A

Marker, Sierra

Swanda, Robert

et al.

Publication Date

2019-07-11

DOI

10.1002/chem.201902223

Peer reviewed

Published in final edited form as:

Chemistry. 2019 July 11; 25(39): 9206–9210. doi:10.1002/chem.201902223.

A Rhenium Isonitrile Complex Induces Unfolded Protein Response-Mediated Apoptosis in Cancer Cells

A. Paden King[‡,a], **Sierra C. Marker**[‡,a], **Robert V. Swanda**[b], **Joshua J. Woods**[c], **Shu-Bing Qian**[b], and **Justin J. Wilson**[a]

[a]Department of Chemistry and Chemical Biology, Cornell University, Ithaca, NY 14853 (USA),

[b]Division of Nutritional Sciences, Cornell University, Ithaca, NY 14853 (USA)

[c]Robert F. Smith School for Chemical and Biomolecular Engineering, Cornell University, Ithaca, NY 14853 (USA)

Abstract

Complexes of the element Re have recently been shown to possess promising anticancer activity via mechanisms of action that are distinct from the conventional metal-based drug cisplatin. In this study, we report our investigations on the anticancer activity of the complex $[Re(CO)_3(dmphen)(p\text{-}tol\text{-}ICN)]^+$ (TRIP) where dmphen = 2,9-dimethyl-1,10-phenanthroline and p-tol-ICN = 4-methylphenyl isonitrile. TRIP was synthesized via literature methods and exhaustively characterized. This compound exhibits potent in vitro anticancer activity in a wide variety of cell lines. Flow cytometry and immunostaining experiments indicate TRIP induces intrinsic apoptosis. Comprehensive biological mechanistic studies demonstrate this compound triggers the accumulation of misfolded proteins, which causes endoplasmic reticulum (ER) stress, the unfolded protein response, and apoptotic cell death. Furthermore, TRIP induces hyperphosphorylation of eIF2α, translation inhibition, mitochondrial fission, and induction of proapoptotic ATF4 and CHOP. These results establish TRIP as a promising anticancer agent based on its potent cytotoxic activity and ability to induce ER stress.

Graphical Abstract

jjw275@cornell.edu.

‡Denotes equal contribution

Supporting information for this article is given via a link at the end of the document. CCDC 1902045 contain the supplementary crystallographic data for this paper. These data can be obtained free of charge from The Cambridge Crystallographic Data Centre.

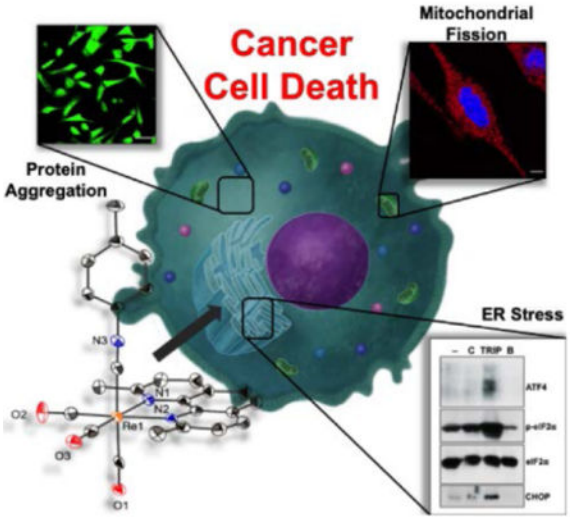

A newly synthesized rhenium tricarbonyl complex kills cancer cells by inducing the accumulation of unfolded proteins, leading to activation of the unfolded protein response and apoptosis.

Keywords

bioinorganic chemistry; cancer; endoplasmic reticulum stress; metallodrug; translation inhibition

The endoplasmic reticulum (ER) is a major regulator of cancer cell proliferation, metastasis, angiogenesis, and chemotherapy resistance.[1] Cancer cells often exhibit higher rates of protein synthesis than non-cancer cells, which raises their ER protein load and leads to higher basal levels of ER stress.[2] To handle this ER stress, cancer cells often employ the unfolded protein response (UPR). The UPR is typically cytoprotective, and its increased activation in cancer cells can cause them to be more virulent and more resistant to chemotherapy.[3] However, acute inductions of high levels of ER stress can shift the UPR to activate apoptosis.[4] The higher basal ER stress levels of cancer cells makes them more susceptible than normal cells to apoptosis induction via overactivation of the UPR. Thus, the development of new chemotherapeutic agents that target the ER is a promising strategy for the treatment of cancer.[5] Recently, several transition metal complexes bearing polypyridyl ligands have been discovered to induce anticancer activity via ER stress and the UPR, suggesting that the exploration of these non-traditional scaffolds may give rise to promising drug candidates.[6–11] In this context, our group has been exploring the anticancer activity of polypyridyl rhenium(I) tricarbonyl complexes.[12–15] Certain members of this class of compounds exhibit potent cytotoxic activity that can be leveraged for their use as anticancer agents.[16–23] Here, we describe our investigation of a new rhenium(I) tricarbonyl complex bearing a chelating polypyridyl ligand and an axial isonitrile ligand as a potent anticancer agent. Our efforts to understand the mechanism of action of this tricarbonyl rhenium isonitrile polypyridyl (TRIP) complex have revealed that it is an effective ER stress-inducing agent with significant antiproliferative activity.

TRIP was synthesized by treating the previously reported complex $[Re(CO)_3(dmphen)OTf]$ with excess 4-methylphenyl isonitrile in tetrahydrofuran (Figure 1). TRIP was fully characterized using ^1H NMR and IR spectroscopy, HR-MS, and X-ray diffraction (Figures S1 and S2, Tables S1 and S2). The purity of the complex was verified via elemental analysis and HPLC (Figure S3, Table S3). The water-soluble complex is luminescent upon irradiation with UVA and blue light and exhibits a luminescence quantum yield of 3% and a lifetime of 1.05 μs in aqueous, air-equilibrated phosphate buffer (Figures S4–S6). The complex is stable indefinitely as a solid and in aqueous solution for over one week (Figures S7 and S8). TRIP is also stable in the presence of millimolar concentrations of glutathione (Figure S9). Based on TRIP's favorable physical properties and high stability, we evaluated its potential as an anticancer agent in vitro.

The cytotoxicity of TRIP was investigated in a panel of cancer and non-cancer cell lines to determine its potential as a therapeutic agent. For comparison, we also evaluated the activities of the established metal-based anticancer drug cisplatin and another potent rhenium anticancer agent that we have previously investigated in our lab, $[Re(CO)_3(dmphen)(OH_2)]^+$ (Neo-Re).[12,15] The concentrations of these complexes required to reduce cell viability to 50% of the control (IC_{50}) are shown in Table 1. In comparison to cisplatin and Neo-Re, TRIP has comparable or greater toxicity in all cancer cell lines tested (Figures S10–S21). Based on its promising anticancer activity, we submitted TRIP for screening in the National Cancer Institute (NCI)-60 cell line panel (Figure S22).[24] The results indicate that TRIP is most potent in melanoma and breast cancer cells lines and least effective in lung and renal cancer cell lines. The activity of TRIP in this cell line panel was compared to drugs in the NCI database via the COMPARE algorithm, which compares the toxicity profiles of drugs to reveal correlations in their activity.[25] Highest correlations were observed for DNA-binding agents chromomycin A3 and actinomycin D and the translation inhibitors pyllanthoside, bruceantin, and didemnin B (Table S4). Notably, the spectrum of activity of TRIP was not correlated to any of the platinum-based drugs, and it exhibits only a moderate correlation (PCC = 0.403) to Neo-Re. The high correlations to established transcription and translation inhibitors indicates that TRIP may act similarly.

To determine the type of cell death induced by TRIP, the cytotoxicity of this compound in A2780 cells was evaluated in the presence of inhibitors of various established cell death pathways. Inhibitors of necroptosis, paraptosis, and ferroptosis did not alter TRIP's activity, but the pan-caspase inhibitor Z-VAD-FMK significantly decreased TRIP's cytotoxicity (Figures S23–S27). Because the activation of caspases is often critical for the execution of apoptosis, this result indicates that TRIP may be inducing apoptosis. To confirm that TRIP induces caspase-dependent apoptosis, we first performed western blots to detect apoptosis markers caspase 3 and cleaved PARP (Figure S28). We further verified this cell death pathway by performing the annexin V assay, which selectivity stains apoptotic cells (Figures S29 and S30). To determine whether TRIP induced apoptosis by the intrinsic pathway, the release of cytochrome *c* from the mitochondria was tracked using flow cytometry (Figure S31). Cytochrome *c* release occurs on the same time scale as apoptosis induction by TRIP, indicating that TRIP induces intrinsic apoptosis.

Given the promising activity of TRIP in a variety of cancer cell lines and its ability to induce intrinsic apoptosis, we explored its intracellular localization and early cellular effects. The localization of TRIP was probed by measuring the colocalization of TRIP luminescence with organelle-specific fluorescent small molecules or fusion proteins. Partial colocalization was observed with the LysoTracker Red dye and GalT-dsRed fusion protein, but the majority of TRIP luminescence was cytosolic (Figure S32). While performing these colocalization studies, we observed that the mitochondrial morphology was noticeably altered in TRIP-treated cells. The mitochondria were significantly rounded and punctate after TRIP treatment, in contrast to the tubular, elongated morphology within untreated cells. Time-lapse microscopy experiments revealed that TRIP induces these changes after only 30 min of treatment in HeLa cells (Figures 2 and S33, Videos 1–6). Although TRIP-treated mitochondria were visually different, mitochondrial polarization experiments with the ratiometric sensor JC-1 indicated that the mitochondria remained functional (Figures S34 and S35), demonstrating that the observed changes might be controlled mitochondrial fission rather than fragmentation. These morphology changes were curtailed in the presence of Mdivi-1, which inhibits dynamin-related protein 1 (Drp1), an essential mediator of fission, confirming that this process is due to mitochondrial fission (Figure 2).[26] Because mitochondrial fission is often associated with autophagy,[27] we examined the expression of LC3, an autophagosome marker,[28] in A2780 cells upon treatment with TRIP. After 24 h, a large increase in LC3II expression relative to LC3I was observed in cells treated with TRIP (Figure S36). Based on these results, it is clear that TRIP induces both autophagy and apoptosis. Because TRIP does not depolarize the mitochondria or cause release of cytochrome *c* on short time scales, we hypothesized that a different organelle, such as the ER, may be the key target of this compound.

Because of the potential connections between mitochondrial fission, autophagy, and ER stress, we explored the effects of the ER stress modulator salubrinal on the cytotoxicity of TRIP in A2780 cells.[29] Salubrinal operates by inhibiting dephosphorylation of the master regulatory protein eukaryotic initiation factor 2α (eIF2α), an integral component of the UPR.[29–32] The presence of salubrinal increases the activity of TRIP by a factor of 4 (Figure 3A). Based on this synergy, we explored the possibility that TRIP was acting to cause phosphorylation of eIF2α. Western blot analysis of A2780 cells treated with TRIP confirms the induction of eIF2α phosphorylation as little as 2 h after exposure (Figures 3B and S37), indicating that this process is one of the first cellular responses. Next, we explored the downstream effects of eIF2α phosphorylation. The most immediate and pronounced effect of eIF2α phosphorylation is the inhibition of translation.[33] To probe whether the levels of phosphorylation induced by TRIP were sufficient to inhibit protein translation, we measured endogenous global translation levels using the puromycin incorporation assay.[34] As early as 2 h post incubation, A2780 cells treated with TRIP incorporated substantially less puromycin compared to the untreated controls, indicating much lower rates of translation (Figure 3C). The role of eIF2α in these processes was confirmed by testing TRIP in a mutant MEF cell line incapable of eIF2α phosphorylation. The mutant cells showed no changes in translation levels after TRIP treatment (Figures S38 and S39).

Hyperphosphorylation of eIF2α can lead to apoptosis via upregulation of the stress-related transcription factors ATF4 and CHOP.[35] We measured the upregulation of these proteins in

response to TRIP treatment and found that both ATF4 and CHOP were upregulated (Figure 3B), linking the observed eIF2α phosphorylation and apoptosis. Phosphorylation of eIF2α also results in cell cycle arrest in the G1 phase.[36] Cells treated with TRIP showed an 18% increase in the population of cells in the G1 phase and a corresponding decrease in the number of cells in the S phase as opposed to untreated cells (Figure S40). Thus, the ability of TRIP to stall cells in the G1 phase is fully consistent with its induction of eIF2α phosphorylation. These results indicate that TRIP induces ER stress, triggering eIF2α phosphorylation and the resulting downstream effects, culminating in cellular apoptosis.

Phosphorylation of eIF2α often occurs due to the accumulation of misfolded proteins. To determine whether the observed phosphorylation was due to protein misfolding, the extent of misfolded protein accumulation induced by TRIP was evaluated using the dye Thioflavin T, (ThT) which fluoresces in the presence of protein aggregates.[37] The fluorescence intensity of ThT increased significantly in HeLa cells treated with TRIP in comparison to untreated cells within 30 min (Figures 3D, S41 and S42, Videos 7 and 8). Given the observation of fast protein aggregation upon treatment with TRIP, the induction of protein misfolding is most likely the cause of the ER stress and activation of the UPR.

A summary of our current understanding of TRIP's mechanism of ER stress induction and the subsequent cellular response is shown in Figure 4. TRIP induces ER stress in less than 30 min after exposure due to the accumulation of misfolded proteins. Misfolded protein accumulation leads to the phosphorylation of eIF2α, which initiates autophagy, shuts down global protein translation, and upregulates ATF4. Prolonged eIF2α phosphorylation and upregulation of ATF4 leads to expression of the proapoptotic protein CHOP, which induces mitochondrial membrane depolarization and release of cytochrome *c*. Cytochrome *c* release then results in caspase activation and initiation of apoptosis. Although we have investigated potential causes of eIF2α phosphorylation, including proteasome inhibition, HSP90 inhibition, and reactive oxygen species generation, we found no evidence that TRIP triggers protein misfolding via these pathways (Figures S43–S47). Recently, a range of diverse metal complexes have been shown to induce ER stress.[7–11,38–47] The major mechanism of action proposed for these agents is through the production of ROS. Only a few studies have discovered metal complexes that induce ER stress in the absence of ROS generation.[9,38,39,48] TRIP's ability to induce ER stress independent of ROS generation indicates that it operates via a different mechanism than many other metallodrugs targeting the ER.

Collectively, these results establish TRIP as a promising anticancer agent that kills cells by causing the accumulation of misfolded proteins. TRIP's favorable physical and photophysical properties, as well as its high potency, make it a candidate for future studies and a platform for the design of more potent analogues. Our current efforts are directed toward synthesizing a variety of related complexes in order to develop a structure-activity relationship and performing proteomics studies to identify TRIP's molecular mechanism of action.

Supplementary Material

Refer to Web version on PubMed Central for supplementary material.

Acknowledgements

This research was supported by the College of Arts and Sciences at Cornell University, the Cornell Technology Licensing Office Cornell Technology Acceleration and Maturation (CTAM) fund, and by the Office of the Assistant Secretary of Defense for Health Affairs through the Ovarian Cancer Research Program under award no. W81XWH-17–1–0097. This work made use of the NMR facility at Cornell University, which is supported, in part, by the NSF under award number CHE-1531632. A. Paden King and R. Swanda thank the National Institute of Health, National Institute of General Medical Sciences, for a Chemical Biology Interface (CBI) Training Grant (grant number T32GM008500). Work in the lab of S.-B. Qian is supported by NIH grants R01GM1222814 and R21CA227917 and by the Howard Hughes Medical Institute (award number 55108556). J. J. Woods is supported by the NSFGRFP (DGE-1650441). We would like to thank the BRC imaging facility at Cornell University for help with flow cytometry experiments. We would also like to thank Prof. Warren Zipfel and Prof. Jeremy Baskin for assistance with the fluorescence decay lifetime measurements and allowing us to use their confocal fluorescence microscope for acquiring all the live cell images, respectively. Ms. Sam Davalos is thanked for assistance in preparing the Table of Contents Figure.

References

[1]. Urra H, Dufey E, Avril T, Chevet E, Hetz C, Trends in Cancer 2016, 2, 252–262. [PubMed: 28741511]

[2]. Vandewynckel Y-P, Laukens D, Geerts A, Bogaerts E, Paridaens A, Verhelst X, Janssens S, Heindryckx F, Van Vlierberghe H, Anticancer Res. 2013, 33, 4683–4694. [PubMed: 24222102]

[3]. Mann MJ, Hendershot LM, Cancer Biol. Ther 2006, 5, 736–740. [PubMed: 16861918]

[4]. Sano R, Reed JC, Biochim. Biophys. Acta - Mol. Cell Res 2013, 1833, 3460–3470.

[5]. Ojha R, Amaravadi RK, Pharmacol. Res 2017, 120, 258–266. [PubMed: 28396092]

[6]. Pracharova J, Vigueras G, Novohradsky V, Cutillas N, Janiak C, Kostrhunova H, Kasparkova J, Ruiz J, Brabec V, Chem. - A Eur. J 2018, 24, 4607–4619.

[7]. Cao R, Jia J, Ma X, Zhou M, Fei H, J. Med. Chem 2013, 56, 3636–3644. [PubMed: 23594206]

[8]. Zou T, Lok C-N, Fung YME, Che C-M, Chem. Commun 2013, 49, 5423–5425.

[9]. Meng X, Leyva ML, Jenny M, Gross I, Benosman S, Fricker B, Harlepp S, Hébraud P, Boos A, Wlosik P, Bischoff P, Sirlin C, Pfeffer M, Loeffler J-P, Gaiddon C, Cancer Res. 2009, 69, 5458–5466. [PubMed: 19549908]

[10]. Nam JS, Kang M-G, Kang J, Park S-Y, Lee SJC, Kim H-T, Seo JK, Kwon O-H, Lim MH, Rhee H-W, Kwon T-H, J. Am. Chem. Soc 2016, 138, 10968–10977. [PubMed: 27494510]

[11]. Suntharalingam K, Johnstone TC, Bruno PM, Lin W, Hemann MT, Lippard SJ, J. Am. Chem. Soc 2013, 135, 14060–14063. [PubMed: 24041161]

[12]. Knopf KM, Murphy BL, MacMillan SN, Baskin JM, Barr MP, Boros E, Wilson JJ, J. Am. Chem. Soc 2017, 139, 14302–14314. [PubMed: 28948792]

[13]. Marker SC, MacMillan SN, Zipfel WR, Li Z, Ford PC, Wilson JJ, Inorg. Chem 2018, 57, 1311–1331. [PubMed: 29323880]

[14]. Konkankit CC, Vaughn BA, MacMillan SN, Boros E, Wilson JJ, Inorg. Chem 2019, 58, 3895–3909. [PubMed: 30793900]

[15]. Konkankit CC, King AP, Knopf KM, Southard TL, Wilson JJ, ACS Med. Chem. Lett 2019, 10, 822–827. [PubMed: 31098006]

[16]. Konkankit CC, Marker SC, Knopf KM, Wilson JJ, Dalton Trans. 2018, 47, 9934–9974. [PubMed: 29904760]

[17]. Simpson PV, Casari I, Paternoster S, Skelton BW, Falasca M, Massi M, Chem. - A Eur. J 2017, 23, 6518–6521.

[18]. Agorastos N, Borsig L, Renard A, Antoni P, Viola G, Spingler B, Kurz P, Alberto R, Chem. - A Eur. J 2007, 13, 3842–3852.

[19]. Kurzwernhart A, Kandioller W, Bartel C, Bächler S, Trondl R, Mühlgassner G, Jakupec MA, Arion VB, Marko D, Keppler BK, et al., Chem. Commun 2012, 48, 4839–4841.

[20]. Imstepf S, Pierroz V, Rubbiani R, Felber M, Fox T, Gasser G, Alberto R, Angew. Chem. Int. Ed 2016, 55, 2792–2795.

[21]. Kottelat E, Chabert V, Crochet A, Fromm KM, Zobi F, Eur. J. Inorg. Chem 2015, 2015, 5628–5638.

[22]. Leonidova A, Pierroz V, Rubbiani R, Heier J, Ferrari S, Gasser G, Dalton Trans. 2014, 43, 4287–4294. [PubMed: 23982882]

[23]. Leonidova A, Gasser G, ACS Chem. Biol 2014, 9, 2180–2193. [PubMed: 25137157]

[24]. Shoemaker RH, Nat. Rev. Cancer 2006, 6, 813–823. [PubMed: 16990858]

[25]. Zaharevitz DW, Holbeck SL, Bowerman C, Svetlik PA, J. Mol. Graph. Model 2002, 20, 297–303. [PubMed: 11858638]

[26]. Cassidy-Stone A, Chipuk JE, Ingerman E, Song C, Yoo C, Kuwana T, Kurth MJ, Shaw JT, Hinshaw JE, Green DR, Nunnari J., Dev. Cell 2008, 14, 193–204. [PubMed: 18267088]

[27]. Niu M, Dai X, Zou W, Yu X, Teng W, Chen Q, Sun X, Yu W, Ma H, Liu P, Transl. Neurosci 2017, 8, 37–48. [PubMed: 28729917]

[28]. Tanida I, Ueno T, Kominami E, Humana Press, Albuquerque, NM, 2008, pp. 77–88.

[29]. Boyce M, Bryant KF, Jousse C, Long K, Harding HP, Scheuner D, Kaufman RJ, Ma D, Coen DM, Ron D, Yuan J, Science 2005, 307, 935–939. [PubMed: 15705855]

[30]. Pakos-Zebrucka K, Koryga I, Mnich K, Ljujic M, Samali A, Gorman AM, EMBO Rep. 2016, 17, 1374–1395. [PubMed: 27629041]

[31]. Teske BF, Wek SA, Bunpo P, Cundiff JK, McClintick JN, Anthony TG, Wek RC, Mol. Biol. Cell 2011, 22, 4390–4405. [PubMed: 21917591]

[32]. DuRose JB, Scheuner D, Kaufman RJ, Rothblum LI, Niwa M, Mol. Cell. Biol 2009, 29, 4295–4307. [PubMed: 19470760]

[33]. Kimball SR, Int. J. Biochem. Cell Biol. 1999, 31, 25–29. [PubMed: 10216940]

[34]. Schmidt EK, Clavarino G, Ceppi M, Pierre P, Nat. Methods 2009, 6, 275–277. [PubMed: 19305406]

[35]. Matsumoto H, Miyazaki S, Matsuyama S, Takeda M, Kawano M, Nakagawa H, Nishimura K, Matsuo S, Biol. Open 2013, 2, 1084–1090. [PubMed: 24167719]

[36]. Brewer JW, Diehl JA, Proc. Natl. Acad. Sci. U. S. A 2000, 97, 12625–12630. [PubMed: 11035797]

[37]. Beriault DR, Werstuck GH, Biochim. Biophys. Acta - Mol. Cell Res 2013, 1833, 2293–2301.

[38]. Chow MJ, Licona C, Pastorin G, Mellitzer G, Ang WH, Gaiddon C, Chem. Sci 2016, 7, 4117–4124. [PubMed: 30155055]

[39]. Chow MJ, Babak MV, Tan KW, Cheong MC, Pastorin G, Gaiddon C, Ang WH, Mol. Pharm 2018, 15, 3020–3031. [PubMed: 29979603]

[40]. Wang F-Y, Tang X-M, Wang X, Huang K-B, Feng H-W, Chen Z-F, Liu Y-N, Liang H, Eur. J. Med. Chem 2018, 155, 639–650. [PubMed: 29935437]

[41]. Wang X, Guo Q, Tao L, Zhao L, Chen Y, An T, Chen Z, Fu R, Mol. Carcinog 2017, 56, 218–231. [PubMed: 27061377]

[42]. Mandal S, Poria DK, Ghosh R, Ray PS, Gupta P, Dalton Trans. 2014, 43, 17463–17474. [PubMed: 25341053]

[43]. Lam T-L, Tong K-C, Yang C, Kwong W-L, Guan X, Li M-D, Kar-Yan Lo V, Lai-Fung Chan S, Lee Phillips D, Lok C-N, Che C-M, Chem. Sci 2019, 10, 293–309. [PubMed: 30746082]

[44]. Zhao J, Li S, Wang X, Xu G, Gou S, Inorg. Chem 2019, 58, 2208–2217. [PubMed: 30675781]

[45]. Kwong W-L, Wai-Yin Sun R, Lok C-N, Siu F-M, Wong S-Y, Low K-H, Che C-M, Chem. Sci 2013, 4, 747–754.

[46]. Huang K-B, Wang F-Y, Tang X-M, Feng H-W, Chen Z-F, Liu Y-C, Liu Y-N, Liang H, J. Med. Chem 2018, 61, 3478–3490. [PubMed: 29606001]

[47]. Wang Y, Hu J, Cai Y, Xu S, Weng B, Peng K, Wei X, Wei T, Zhou H, Li X, Liang G, J. Med. Chem 2013, 56, 9601–9611. [PubMed: 24274598]

[48]. Tardito S, Isella C, Medico E, Marchiò L, Bevilacqua E, Hatzoglou M, Bussolati O, Franchi-Gazzola R, J. Biol. Chem 2009, 284, 24306–19. [PubMed: 19561079]

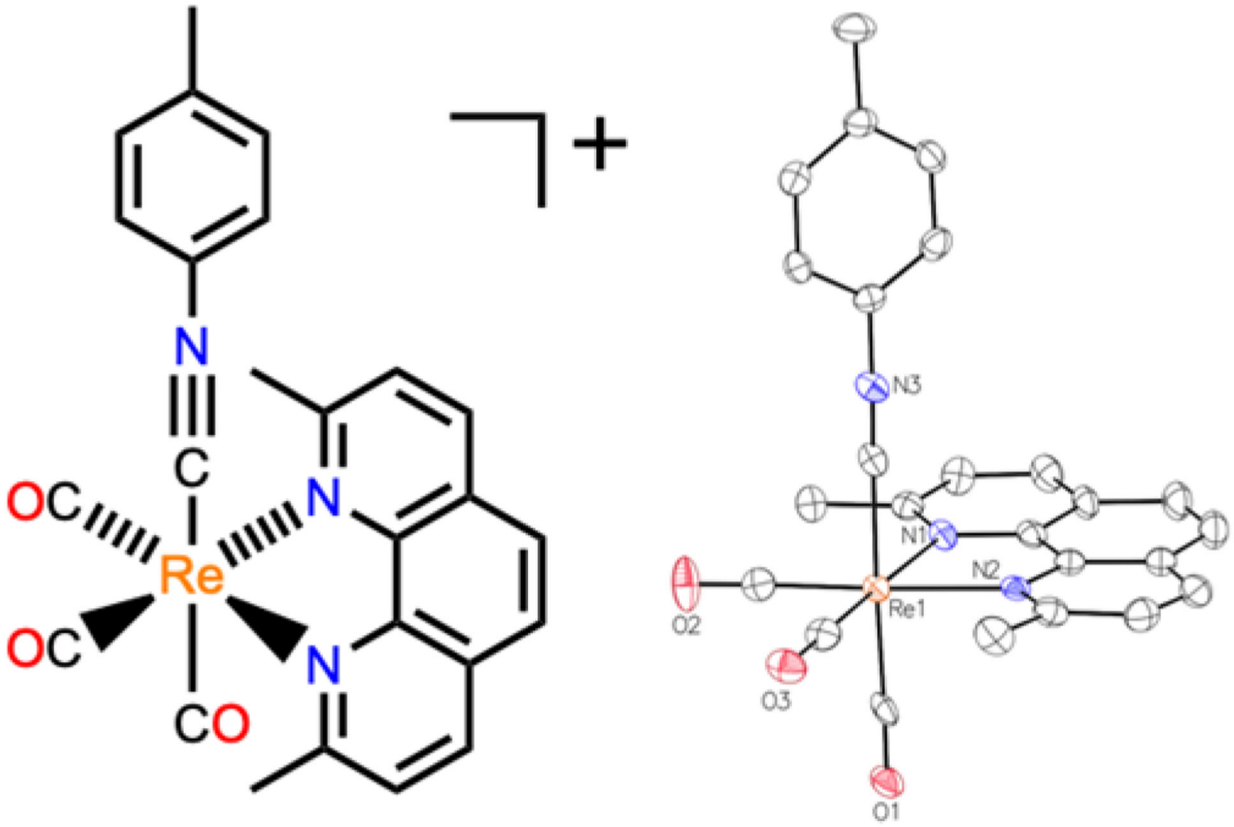

Figure 1.
Diagram of TRIP (left) and its X-ray crystal structure (right). Ellipsoids are drawn at 50% probability. Hydrogen atoms and the counterion are omitted for clarity.

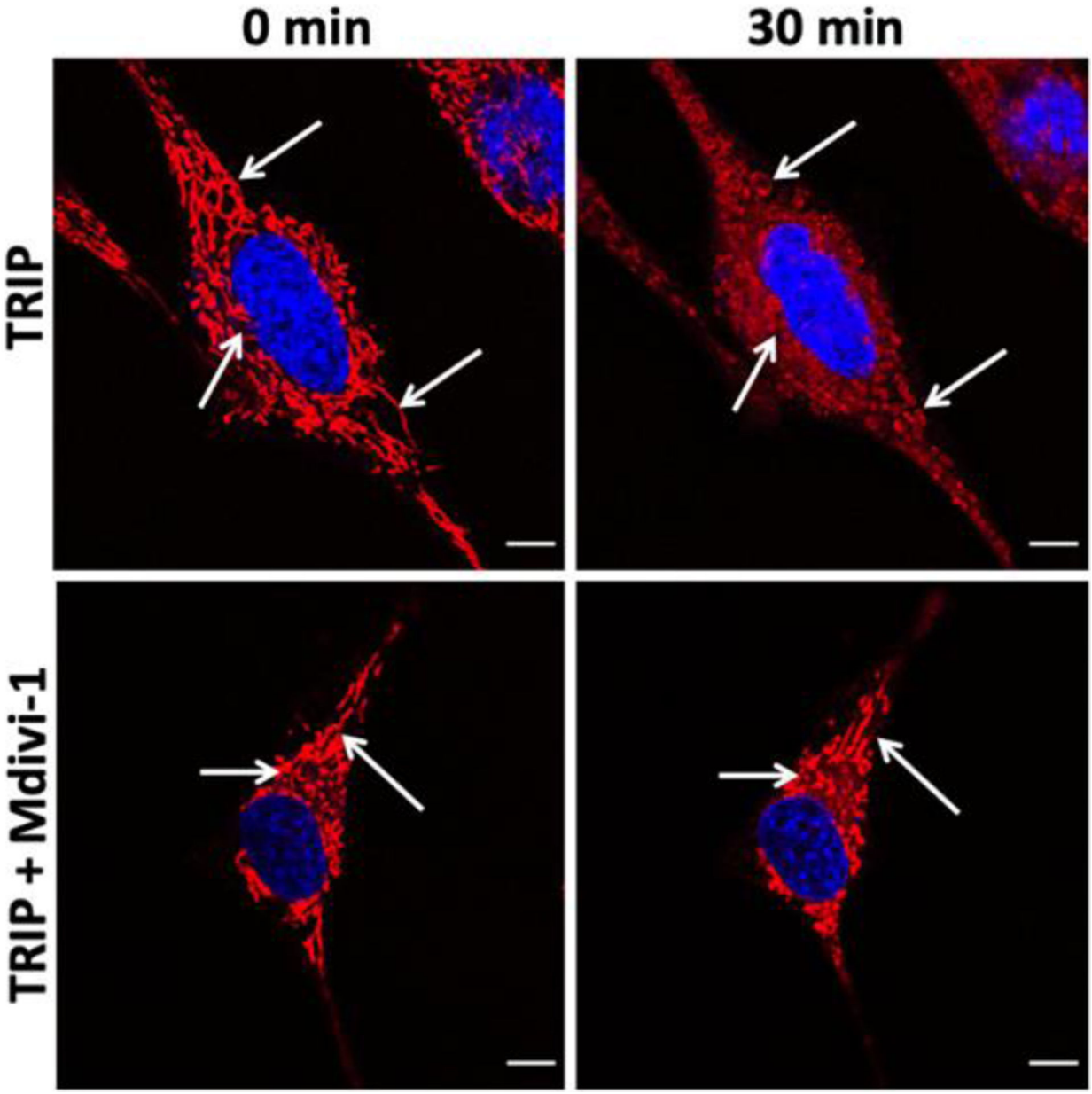

Figure 2.

HeLa cells stained with MitoTracker Red and Hoechst dye treated with TRIP (5 μM) for 0 and 30 min (top panels). HeLa cells stained with MitoTracker Red and Hoechst dye cotreated with TRIP (5 μM) and Mdivi-1 (50 μM) for 0 and 30 min (bottom panels). Scale bar = 10 μm.

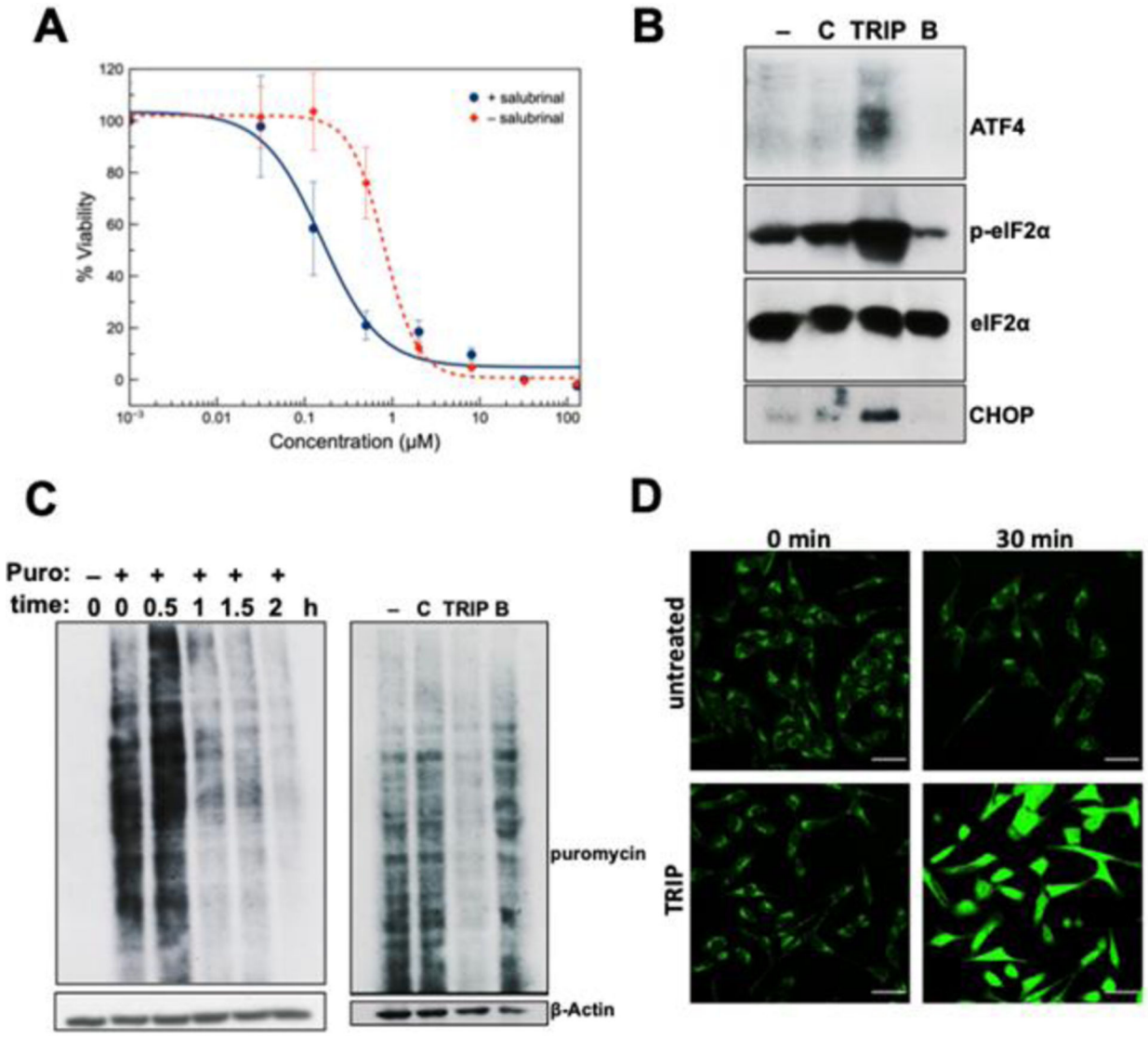

Figure 3.

(**A**) Dose-response curve of A2780 cells treated with TRIP in the presence of 25 μM salubrinal (blue) or absence of salubrinal (red). (**B**) Western blot of untreated (–), cisplatin (C, 10 μM), TRIP (5 μM), or bortezomib (B, 25 nM) for 24 h in A2780 cells. (**C**) Western blot of A2780 cells incubated with TRIP (5 μM) over 0, 0.5, 1, 1.5, and 2 h with puromycin (10 min, left blot) and A2780 cells untreated (–), cisplatin (C, 10 μM), TRIP (5 μM), or bortezomib (B, 25 nM) treated for 24 h with puromycin (10 min, right blot). (**D**) Confocal microscopy images of HeLa cells treated with ThT (5 μM) at 0 and 30 min in the absence (top panels) and the presence (bottom panels) of TRIP (5 μM) at 0 and 30 min. Scale bar = 50 μm.

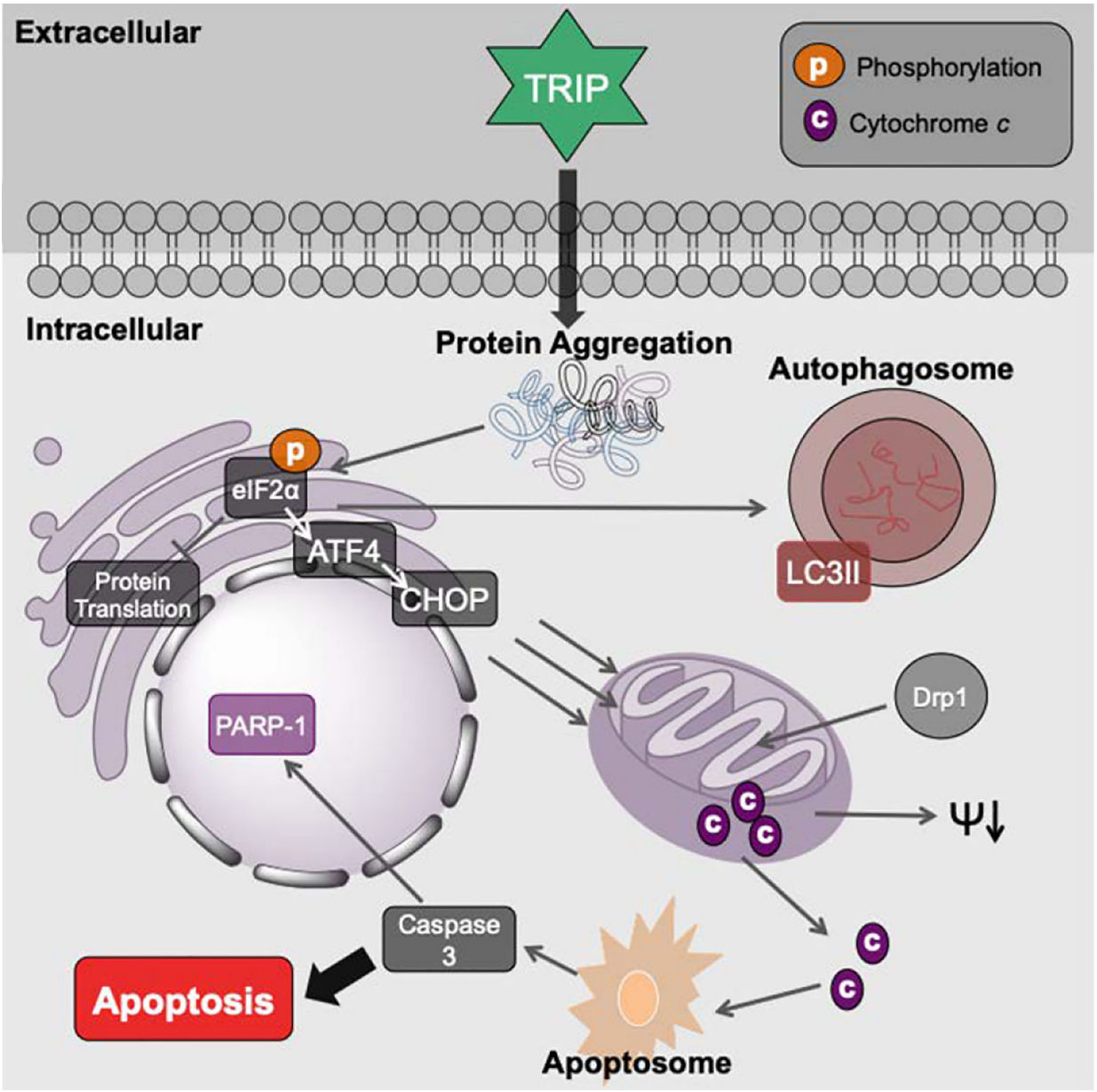

Figure 4.
Proposed mechanism of ER-stress and apoptosis induction by TRIP.

Table 1.

IC_{50} values of TRIP, Neo-Re, and cisplatin in cancer and non-cancer cell lines.

Compound	IC_{50} (μM)				
	A2780 (ovarian cancer)	A2780 CP70 (cisplatin-resistant ovarian cancer)	HeLa (cervical cancer)	A549 (lung cancer)	HEK293 (kidney)
TRIP	1.7 ± 0.7	1.9 ± 1	1.4 ± 0.2	1.4 ± 0.6	1.9 ± 0.2
Neo-Re	5.7 ± 0.6	6.0 ± 0.2	4.4 ± 1.3	7.7 ± 2.4	9.0 ± 0.3
Cisplatin	1.3 ± 0.1	12 ± 3	6.6 ± 0.7	5.6 ± 0.5	1.7 ± 0.2